Alternative mechanisms alter the emergent properties of self-organization in mussel beds

Liu, Quan-Xing; Weerman, Ellen J.; Herman, Peter M. J.; Olff, Han; van de Koppel, Johan

Published in:
Proceedings of the Royal Society of London. Series B, Biological Sciences

DOI:
10.1098/rspb.2012.0157

Publication date:
2012

ONLINE SUPPLEMENTARY MATERIAL: Appendix A

Alternative mechanisms alter the emergent properties of self-organization in mussel beds

Quan-Xing Liu[1,2,3,§], Ellen J.Weerman[3], Peter M.J. Herman[1,2], Han Olff[3], and Johan van de Koppel[1,3]

1. Department of Spatial Ecology, Royal Netherlands Institute for Sea Research, P.O. Box 140, 4400 AC Yerseke, The Netherlands;

2. Netherlands Institute of Ecology (NIOO-KNAW), Droevendaalsesteeg 10, 6708 PB Wageningen, The Netherlands.

3. Community and Conservation Ecology, Centre for Ecological and Evolutionary Studies, University of Groningen, P.O. Box 11103, 9700 CC Groningen, The Netherlands;

Model parameter choice and dimensions

Here we present a table of the symbols, their interpretation, units, values, and sources as used in the model (Table 1). Below, we present the results of a detailed bifurcation analysis of the dimensionless model.

Table A1: Symbols, interpretation, units, values, and sources used in the decreased losses feedback (DLF) model and sediment accumulation feedback (SAF) models

Symbol	Interpretation	Unit	Value	Source
DLF model				
k_M	Half saturation constant of mussel mortality	g/m^2	150	[8]
SAF model				
f	Exchange coefficient between surface and bottom	1/h	100	Estimated
A_{up}	Concentration of algae in the upper water layer	g/m^3	1.5	[2]
c	Maximum depletion coefficient	m^3/g/h	1.0	[6; 5]

k_S	Half-saturation constant of sediment	—	20.0	Estimated
V	Velocity of tidal flow	m/h	360.0	[1]
e	Conversion constant of ingested algae to mussel production	g/g	0.02	[7; 3]
d_M	Maximal mortality rate per unit time	g/h	0.005	Estimated
D_M	Diffusion coefficient of mussels	m^2/h	0.0005	Estimated
k_1	Production of mud per capital mussels	m/g/h	0.0001	[3]
d_S	Erosion rate of sediment	m/h	0.005	[10]
D_S	Diffusion coefficient of sediment	m^2/h	0.0005	[4]
g	Uptake contrast between flat mussel and hummock	—	0.1	Estimated

Analyses of the sediment accumulation model

Dimensionless forms and scaling

Our model is based on the following reaction-diffusion partial differential equations:

$$\frac{\partial A}{\partial T} = f(A_{\mathrm{up}} - A) - c\Big(\frac{S + k_S g}{S + k_S}\Big) AM + V\frac{\partial A}{\partial X} \tag{A1}$$

$$\frac{\partial M}{\partial T} = ec\Big(\frac{S + k_S g}{S + k_S}\Big) AM - d_{\mathrm{M}} M + D_{\mathrm{M}}\nabla^2 M \tag{A2}$$

$$\frac{\partial S}{\partial T} = k_1 M - d_S S + D_S\nabla^2 S. \tag{A3}$$

The model can greatly be simplified by the following non-dimensionalisation

$$t = d_M T,\ x = \sqrt{d_M/D_M}X,\ y = \sqrt{d_M/D_M}Y,$$

$$a = \frac{d_M}{fA_{up}}A,\ m = \tfrac{k_1}{d_M k_S}M,\ \ s = k_S^{-1}S. \tag{A4}$$

Then, we can obtain the dimensionless equations:

$$\frac{\partial a}{\partial t} = 1 - \alpha a - \beta\frac{s + \eta}{1 + s}am + \nu\frac{\partial a}{\partial x} \tag{A5}$$

$$\frac{\partial m}{\partial t} = \delta\frac{s + \eta}{1 + s}am - m + \Big(\frac{\partial^2}{\partial x^2} + \frac{\partial^2}{\partial y^2}\Big)m \tag{A6}$$

$$\frac{\partial s}{\partial t} = m - \theta s + D\Big(\frac{\partial^2}{\partial x^2} + \frac{\partial^2}{\partial y^2}\Big)s, \tag{A7}$$

where $\alpha = f/d_M$, $\beta = ck_S/k_1$, $\eta = g$, $\nu = V/\sqrt{d_M D_M}$, $D = D_S/D_m$, $\theta = d_S/d_M$, and $\delta = \frac{ecfA_{\rm up}}{d_M^2}$. In applications, the main dimensional parameters of interest are the algae supply f, mussel loss d_M, advection of tidal flow V, and sediment deposition d_S; note that mussel loss will vary depending on the extent of grazing and aggregation of mussels. These four parameter appear in the dimensionless quantities δ, θ and ν, respectively. Therefore, we can study the dimensionless equation (A5)—(A7), focusing on the conditions for patterning and the way in which the patterns vary with these three parameters. Derivation of parameter ranges based on Table yields $\alpha = 50.0 \sim \mathcal{O}(10^1 - 10^2)$, $\beta = 200.0 \sim \mathcal{O}(10^2)$, $\nu = 360.0 \sim \mathcal{O}(10^2 - 10^3)$, $D \geq 1 \sim \mathcal{O}(1 - 10)$, $\delta > 100 \sim \mathcal{O}(10^2)$ and $\theta = 2.5 \sim \mathcal{O}(0 - 10^1)$. To accelerate the simulations, we have multiplied parameters D, V, and theta (please fill in the correct symbols) by a factor 1000. Numerical analysis revealed that this does not alter the relative predictions of the model. Parameter values in dimensionless equation (A5) — (A7) are $D = 1.0$, $\nu = 360.0$, $\theta = 2.5$,with δ as a resource source, allowed to vary.

Steady-state solution and properties of the pattern solutions

The system (A5-A7) has three uniform solutions, one with trivial mussel and sediment:

$$[a_0, m_0, s_0] = [1/\alpha, 0, 0], \tag{A8}$$

and two nontrivial spatially homogeneous steady states arising from a saddle node bifurcation. They are solutions of the system

$$s_\pm = \frac{\Gamma \pm \sqrt{\Gamma^2 - 4\beta\theta\Phi}}{2\beta\theta}, \quad m_\pm = \theta s_\pm, \quad a_\pm = \frac{1 + s_\pm}{\delta(s_\pm + \eta)}, \tag{A9}$$

where $\Gamma = \delta - \alpha - \beta\theta\eta$, $\Phi = \alpha - \delta\eta$ here δ is a function of parameter $A_{\rm up}$. These three uniform solutions, however, exist only for a certain range of values, $\delta > \delta_{SN}$; in this range, both states (a_0, m_0, s_0) and (a_+, m_+, s_+) are stable, defining a *bistability* region, as shown in Figure 4B.

From an ecological point of view, a key issue is how ecosystem functioning depends on parameters values. Van de Koppel et al [8] studied this question in detail by assuming that the mussel patterns are controlled by the concentration of algae in the upper water layer A_{up}. The pattern solutions can be analyzed using the method of periodic travelling wave solutions [9]. However, determination of periodic traveling wave stability, even numerically, is a notoriously difficult problem. In this section, we investigate numerically the existence and stability of patterns with the approach of discretising the PDEs (A1)—(A3) in space. Our approach is to use the bifurcation package AUTO-07p to study the pattern PDEs (A1)—(A3). To do this, the most natural bifurcation parameter is the algae concentration, $A_{\rm up}$. The results of Figure 4 give a

detailed understanding of the existence of patterned solutions, as a function of the model parameter A_{up}. The discretized version of PDEs is given as:

$$\partial A_i/\partial t = f(A_{up} - \alpha A_i) - \mathcal{G}(S_i)A_i M_i + V(A_{i+1} - A_i)/\Delta X \quad \text{(A10)}$$

$$\partial M_i/\partial t = e\mathcal{G}(S_i)A_i M_i - d_M M_i + D_M(M_{i+1} - 2M_i + M_{i-1})/\Delta X^2 \quad \text{(A11)}$$

$$\partial S_i/\partial t = k_1 M_i - d_S S_i + D_S(S_{i+1} - 2S_i + S_{i-1})/\Delta X^2, \quad \text{(A12)}$$

$(i = 1, \cdots, N)$. For simplicity, we assume periodic boundary conditions $A_0(t) = A_N(t)$, $M_0(t) = M_N(t)$, $S_0(t) = S_N(t)$. We studied system (A10)—(A12) using the bifurcation AUTO07p, with the objective of determining the bifurcation diagrams such as those shown in Fig.S1, but with additional information about different branches and pattern stability.

For any discretization that is sufficiently fine to be of practical use, (A10)—(A12) are a large system of equations, and studying patterned solutions using AUTO-07p is a major computational challenge. Therefore, we have focused on pattern variation with just one of the four parameters, the algae concentration A_{up}, with the values of f, d_M and e fixed as listed in Table A1, respectively. We used $N = 50$, which gives 150 equations in Eqs.(A10)—(A12), with a spatial grid length $\Delta X = 3$. This gives a discrete representation of the model equations on a domain of length 150, which is large enough to capture a range of pattern behavior.

For sufficiently large values of A_{up}, there are no patterned solutions, and the homogeneous steady state $A_i = A$, $M_i = M$ and $S_i = S$ $(i = 1, \cdots, N)$ is stable as a solution of (A10)—(A12). As δ decreased, the steady state becomes unstable via a Hopf bifurcation at $A_{\text{up}} \approx 0.9$ (Figure S1A). The branch of periodic solutions emanating from this Hopf bifurcation is spatially as well as temporally periodic, with a wavelength of 10 space points. As A_{up} is decreased further, the homogeneous steady state undergoes a series of additional Hopf bifurcations. At each of these, a branch of periodic solutions emanates, corresponding to a pattern of a particular spatial mode, as shown in Figure S1. Here, we show the amplitude of the homogeneous steady state from which the spatial pattern branches bifurcate. In brief, we use the measurement of $\mathcal{N} = \frac{1}{L}\sqrt{\int_L \left(A^2(x) + M^2(x) + S^2(x)\right)dx}$ to plot the bifurcation graph. The solution branches with different spatial modes arise via separate Hopf bifurcations (Figure S1).

Following the same method, we can obtain the spatial solution and bifurcation on reduced losses model, are shown in Fig.S1C and D respectively.

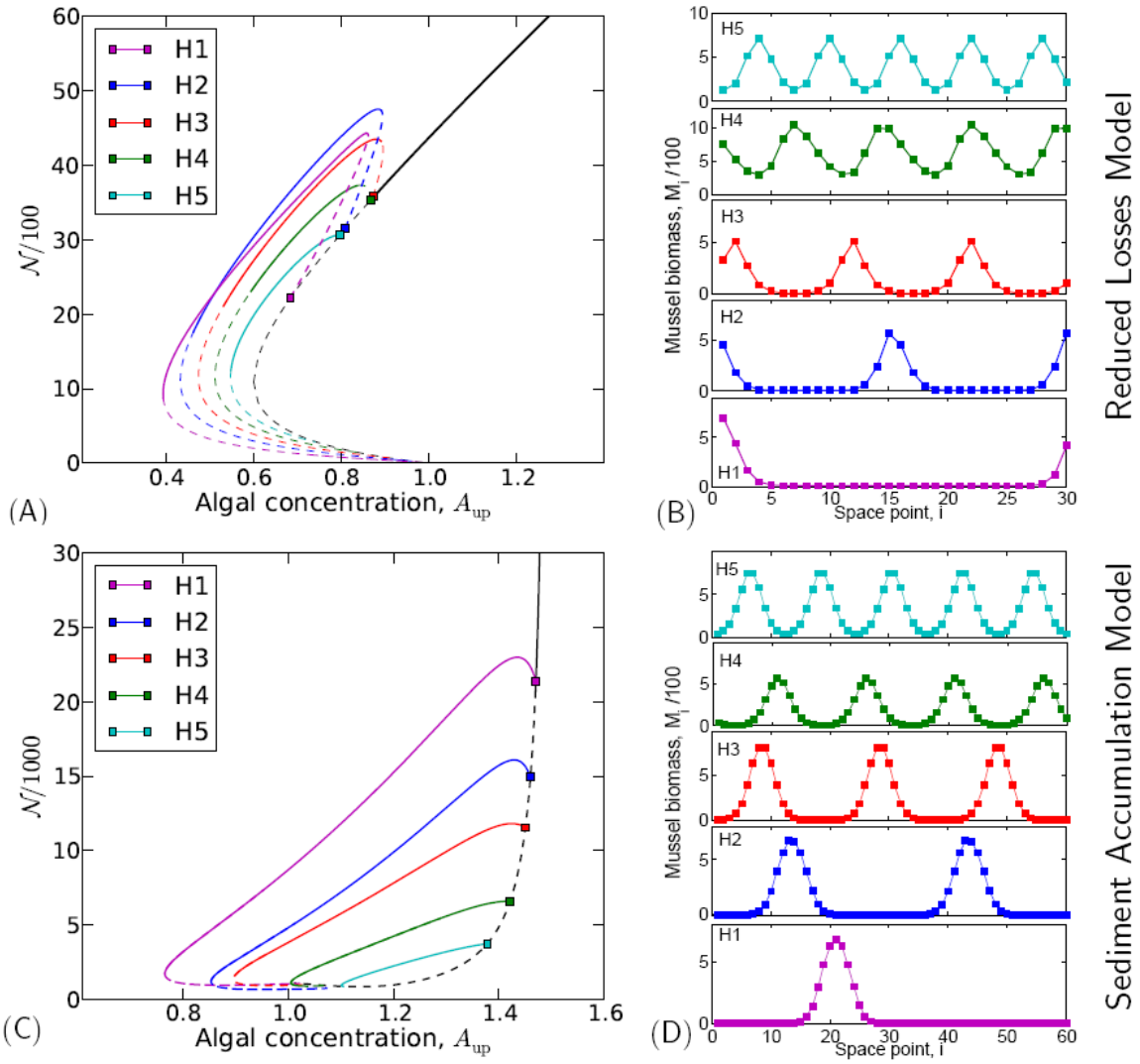

Figure S1: Bifurcation diagram of patterned solutions on the discretised model equations. Solid lines correspond to stable patterned solutions and dashed lines correspond to unstable solutions. Typical spatial profiles of the solutions on the discretized version PDEs related to various branches. (A) and (B) showing results of spatial bifurcation and pattered solutions on sediment accumulation model. (C) and (D) showing the results of spatial bifurcation and pattered solutions on reduced losses model.

Relative accumulation model

The model presented in the main text assumes a direct relation between absolute sediment accumulation (e.g., elevation) and mussel uptake and growth. It is well conceivable that not absolute elevation, but rather the elevation relative to the surrounding sediment determines the increase in uptake and growth of the mussels. In this case, an increase in sediment accumulation over an homogeneous bed would not affect mussel growth. To check robustness of our results in

an alternate formulation of the effects of sediment accumulation, we have constructed a model where we replace S with $S/\bar{S}$ in the feedback function, $\mathcal{G}(S/\bar{S})$, where $\bar{S} = \frac{1}{\Omega}\int_{\Omega} S(r,T)dr$ denotes the average accumulation of sediment over the entire mussel habitat Ω. The parameters are the same as previous studies, apart from the half-saturation constant of sediment, $k_S = 1.0$. Figure S2C shows that very similar patterns are found as in the two models described in the main text. We then performed a bifurcation analysis as was described above for the absolute sediment accumulation model. The results of this are presented in figure S2 below. The bifurcation analysis reveals the relative accumulation model reveals that no bi-stable behavior is found in the relative sedimentation model, but that the bifurcation patterns with regard to pattern formation is very similar. Moreover, similar results are found with respect to the emergent properties of pattern formation on average biomass and recovery time after 10% perturbation as shown in Fig.S2.

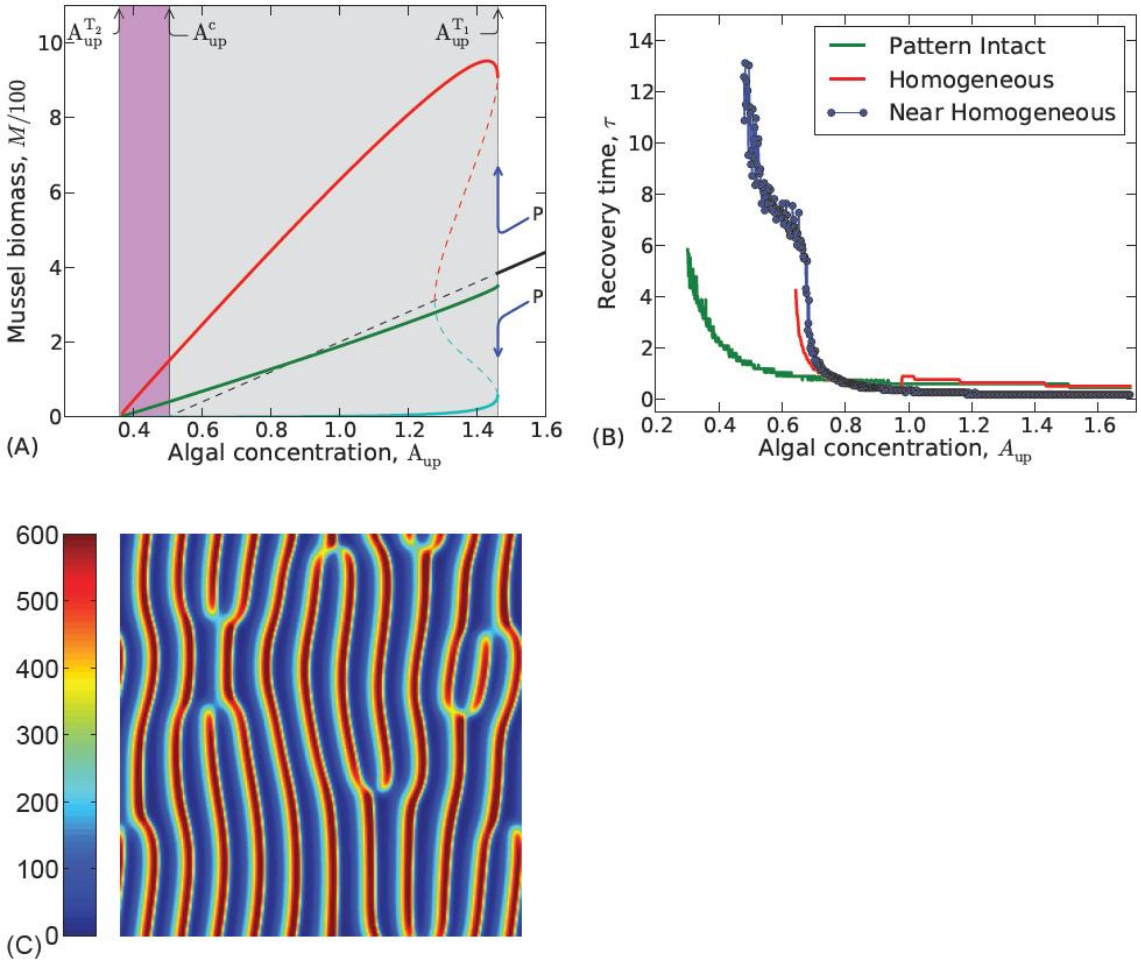

Fig.S2: Results of the relative sediment accumulation model. Panel A present a bifurcation analyses with respect to parameter A_{up}, panel B presents recovery time after a 10% decrease in

biomass (B), and panel C present an example of a spatial pattern (A_{up}=1.2, see table A1 for other parameters).

References

[1] A. G. BRINKMAN, N. DANKERS, and M. VAN STRALEN, 'An analysis of mussel bed habitats in the Dutch Wadden Sea', *Helgoland Mar Res* (1) 56 (2002) 59-75.

[2] G. C. CADEE and J. HEGEMAN, 'Phytoplankton in the Marsdiep at the end of the 20th century; 30 years monitoring biomass, primary production, and Phaeocystis blooms', *J Sea Res* (2) 48 (2002) 97-110.

[3] B. E. COLE, J. K. THOMPSON, and J. E. CLOERN, 'Measurement of Filtration-Rates by Infaunal Bivalves in a Recirculating Flume', *Mar Biol* (2) 113 (1992) 219-225.

[4] M. O. GREEN and G. COCO, 'Sediment transport on an estuarine intertidal flat: Measurements and conceptual model of waves, rainfall and exchanges with a tidal creek', *Estuar Coast Shelf S* (4) 72 (2007) 553-569.

[5] H. U. RIISGARD, 'On measurement of filtration rates in bivalves - the stony road to reliable data: review and interpretation', *Mar Ecol-Prog Ser* 211 (2001) 275-291.

[6] H. SCHOLTEN and A. C. SMAAL, 'Responses of Mytilus edulis L. to varying food concentrations: testing EMMY, an ecophysiological model', *J Exp Mar Biol Ecol* (1-2) 219 (1998) 217-239.

[7] A. A. SUKHOTIN, D. ABELE, and H. O. PORTNER, 'Growth, metabolism and lipid peroxidation in Mytilus edulis: age and size effects', *Mar Ecol-Prog Ser* 226 (2002) 223-234.

[8] J. VAN DE KOPPEL, M. RIETKERK, N. DANKERS, and P. M. J. HERMAN, 'Scale-dependent feedback and regular spatial patterns in young mussel beds', *American Naturalist* (3) 165 (2005) E66-E77.

[9] R. H. WANG, Q. X. LIU, G. Q. SUN, Z. JIN, and J. VAN DE KOPPEL, 'Nonlinear dynamic and pattern bifurcations in a model for spatial patterns in young mussel beds', *Journal of the Royal Society Interface* (37) 6 (2009) 705-718.

[10] J. WIDDOWS, J. S. LUCAS, M. D. BRINSLEY, P. N. SALKELD, and F. J. STAFF, 'Investigation of the effects of current velocity on mussel feeding and mussel bed stability using an annular flume', *Helgoland Mar Res* (1) 56 (2002) 3-12.

ONLINE SUPPLEMENTARY MATERIAL: Appendix B
Alternative mechanisms alter the emergent properties of self-organization in mussel beds

Quan-Xing Liu, Ellen Weerman, Peter Herman, Han Olff, and Johan van de Koppel

February 21, 2012

1 The effect of the perturbation intensity on critical slowing down

In order to detect the effect of the intensity of the perturbation on the phenomenon of critical slowing down (see main text for a definition), we have checked three different perturbations under the same condition, by reducing biomass by 50% and 10%, respectively. They exhibit qualitatively similar result. The typical results of 50% and 10% reduction of biomass are shown in Fig.S1 and in Fig.4 in the main text. For the spatial patterned states, there is a striking absence of the critical slowing down in the reduced losses feedback model. Thus, critical slowing down depends critically on the involved mechanism explaining the observed spatial patterns, and it cannot be concluded without thorough experimental testing of the mechanisms underlying the observed patterns that critical slowing down is a universal phenomenon.

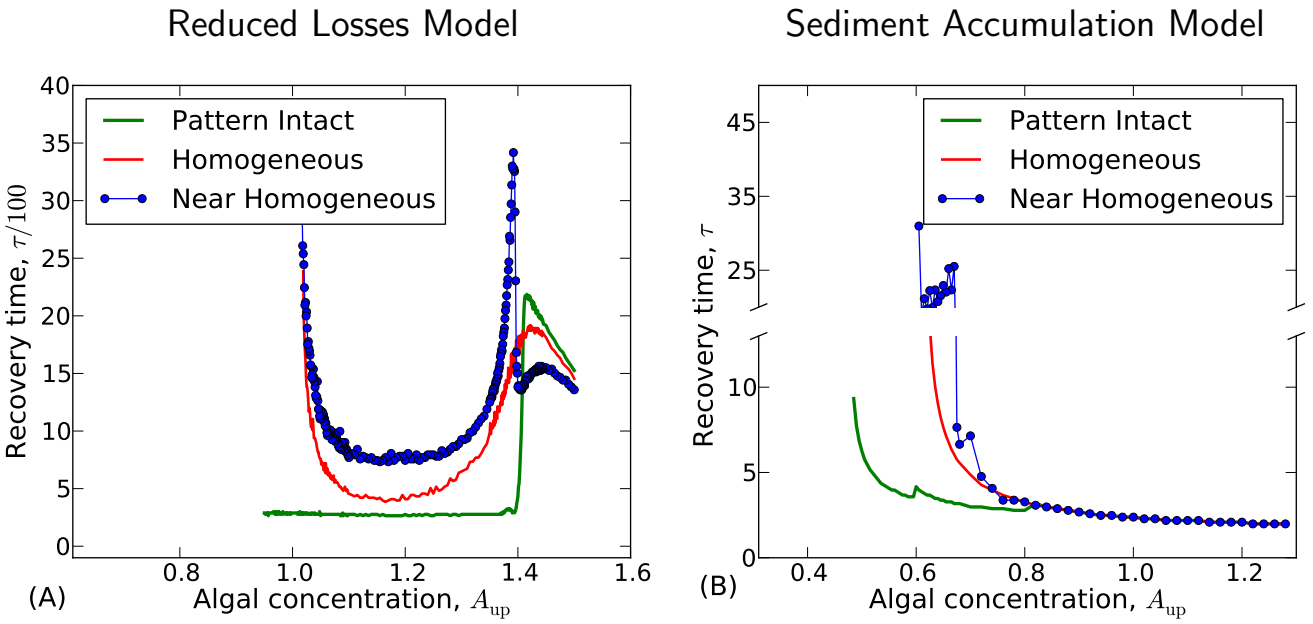

Figure S3. Recovery times following perturbation of the two alternate mechanistic models of pattern formation, using a 50% reduction in biomass for both reduced losses model (A) and sediment accumulation model (B). The parameters are the same as the Fig.5 in the main text.